

Measurement of the $^{12}\text{C}(p, \pi^0)^{13}\text{N}$ reaction by recoil detection

J. Homolka, W. Schott, W. Wagner, and W. Wilhelm
Physik Department, Technische Universität München, Germany

M. Saber and R. E. Segel
Northwestern University, Evanston, Illinois 60208

R. D. Bent, M. Fatyga, and R. E. Pollock
Indiana University Cyclotron Facility, Bloomington, Indiana 47408

P. Kienle
Gesellschaft für Schwerionenforschung, Darmstadt, Germany

K. E. Rehm
Argonne National Laboratory, Argonne, Illinois 60439
 (Received 17 October 1991)

Differential cross sections for the neutral pion production reaction $^{12}\text{C}(p, \pi^0)^{13}\text{N}_{g.s.}$ have been measured at 153.5, 166.1, 186.0, and 204.0 MeV bombarding energy using recoil detection. The shape of the angular distribution agrees well with that of the mirror reaction $^{12}\text{C}(p, \pi^+)^{13}\text{C}_{g.s.}$. Isospin invariance predicts for the ratio of the cross sections $\sigma(p, \pi^+)/\sigma(p, \pi^0) = 2$. At 153.5, 166.1, and 186.0 MeV, where (p, π^+) cross sections have been reported previously by other groups at the same reduced pion momentum $\eta = p_\pi/m_\pi c = 0.34, 0.55, 0.78$, the ratio of the total cross sections is 2.02 ± 0.14 , 3.14 ± 0.12 , and 2.12 ± 0.16 , respectively. The (p, π^0) cross section at 166 MeV is therefore 1.57 ± 0.06 times larger than expected. For $T_p < 160$ MeV, the experimental cross sections are larger than predicted by a phase space and Coulomb barrier penetration calculation that fits the higher-energy data. Differential cross sections were also obtained for the $^{12}\text{C}(p, \pi^-)^{13}\text{O}$ reaction, and upper limits set for differential cross sections for radiative capture to the ground state of ^{13}N .

PACS number(s): 25.40.Qa

INTRODUCTION

Proton-induced pion production leading to a low-lying nuclear state is a process involving large momentum transfer, q , even close to threshold. For the $^{12}\text{C}(p, \pi^0)^{13}\text{N}_{g.s.}$ reaction at threshold ($T_p = 145$ MeV) $q = 2.5 \text{ fm}^{-1}$. This type of reaction is therefore sensitive to nuclear dynamics at short distances.

In recent years, several microscopic models of the $A(p, \pi)A + 1$ reaction have been developed [1,2]. While considerable (p, π^+) data are available, the present work represents the first extensive study of the (p, π^0) reaction on a complex nucleus.

Data on the $^{12}\text{C}(p, \pi^+)^{13}\text{C}$ reaction have been obtained by several groups using magnetic spectrometers to analyze the pion spectra [3–10]. A direct measurement of π^0 's is very difficult. For this reason in the present work the recoiling ions instead of the pions were measured. In addition, with this method the cross sections for the exclusive production of neutral and charged pions can be obtained from one set of data.

EXPERIMENT

The recoils from the $^{12}\text{C}(p, \pi^{0(+)})$ reaction are confined to a cone with an opening angle of 7.4° (6.9°)

at $T_p = 166$ MeV, widening to 11.4° (11.2°) at 200 MeV. Because the recoils are so confined in the laboratory system, they can be detected with high efficiency by a magnetic spectrometer having a moderate solid angle. This method allows the measurement of very small cross sections as was demonstrated in a study of the $^{12}\text{C}(^3\text{He}, \pi^+)^{15}\text{N}$ reaction [11,12], where $\sigma_t < 30$ pb at 170 MeV bombarding energy. Since ^{13}N has no bound excited states, only one ^{13}N recoil group from the $^{12}\text{C}(p, \pi^0)$ reaction has to be considered. There are, however, three particle stable excited states in ^{13}C and with a target thick enough to produce sufficient yield ($192 \mu\text{g}/\text{cm}^2$ was used in the present work) the energy loss of the recoil ions in the target makes it impossible to resolve the ground-state group from the others. The (p, π^+) transitions to the individual ^{13}C states have been resolved, however, in measurements where the pion has been detected.

The experimental method and apparatus have been described previously [13]. By using a magnetic spectrometer, which measures $p/Q = Am_n v/Q$, where p is the momentum, Q the atomic charge, A the atomic number, and m_n the nucleon mass, in combination with a time-of-flight measurement of velocity (v), the ratio A/Q can be determined. The nuclear charge Z is obtained from an energy-loss measurement ($\Delta E/\Delta x$). Since Q , Z , and A are all integers, with $Q \leq Z$ and only certain

(Z, A) combinations possible, these three measurements ($p/Q, v$, and $\Delta E/\Delta x$) are usually sufficient to uniquely determine Z, A , and Q and, therefore, p . For reactions leading to a two-body final state, the recoil products lie on an ellipse in the (p, θ) plane, where θ is the recoil emission angle.

Protons were accelerated to laboratory kinetic energies of 153.5, 166.1, 186.0, and 204.0 MeV in the Indiana University Cyclotron Facility and transported and focused onto a 2 mm diameter spot on a $192 \mu\text{g}/\text{cm}^2$ carbon foil target located in the target chamber of the quadrupole-quadrupole-split-dipole (QQSP) magnetic spectrometer. The energy and angle ranges, and charge state fractions of the ^{13}N recoils are given in Table I. The QQSP has a momentum acceptance of $0.82 < p/p_0 < 1.37$, where p_0 is the central momentum. The angular acceptance was ± 100 mrad and ± 50 mrad in the horizontal (bend) and vertical planes, respectively, while the momentum resolution was $\Delta p/p = 10^{-3}$.

After traversing the QQSP magnets, the recoil ions passed through two transmission-type position-sensitive parallel plate avalanche counters (PPAC's), each with an active area of $60 \times 5 \text{ cm}^2$. The first PPAC was located at the focal plane of the spectrograph and the second PPAC 12 cm further back. After passing through the second PPAC the ions entered a proportional counter (PC) whose purpose was to measure $\Delta E/\Delta x$. The first PPAC was separated from the QQSP vacuum chamber, and the second PPAC from the proportional counter, by $260 \mu\text{g}/\text{cm}^2$ aluminized mylar foils. The cathodes of the PPAC's were also foils of this same thickness, while all other electrodes were wire grids with a transmission of about 99%. The momentum per unit charge, p/Q , and the emission angle, θ , of the recoil ions were determined by measuring the position (x) at the spectrograph focal plane as well as the angle (α), relative to the normal to the focal plane. In the absence of aberrations both p and x and θ and α are linearly related:

$$\frac{p}{p_0} = Ax + B \quad (1)$$

where x is in meters, and

$$\theta = \frac{(\alpha - \alpha_0)}{R_{22}} + \beta. \quad (2)$$

The offset angle, β , is the angle between the proton beam and the QQSP axis and was 4.85° for the present measurements.

Investigations [10] of the optics of the QQSP have

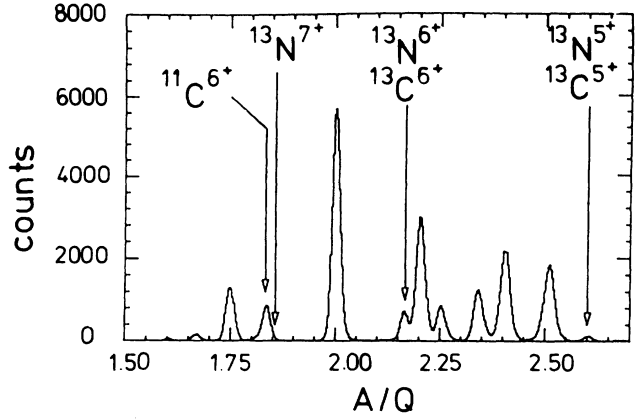


FIG. 1. Spectrum of A/Q at $T_p = 186$ MeV.

shown that the linear relation is adequate for the angular magnification but that higher-order terms must be included if the momentum is to be determined to better than about 1%.

By dividing p/Q by the ion velocity v_1 (determined from the time of flight, t_1 , through the spectrometer), A/Q could be determined to about 1%. The 150–200 ns flight time of the ^{13}N ions exceeded the time between successive cyclotron beam bursts (~ 60 ns) giving rise to a discrete ambiguity in the A/Q determination. This ambiguity was removed by measuring the flight time between the two PPAC's, which determined the velocity to $\sim 10\%$, an accuracy sufficient to remove the ambiguity in the flight time through the QQSP. The atomic number Z of the higher-energy recoil ions was determined by measuring the energy loss in a $60 \times 5 \text{ cm}^2$ gas PC mounted immediately behind the second PPAC. For the Z determination of the recoils that did not have enough energy to penetrate the PC, the energy loss in the foils of the first PPAC, as determined by the time of flight between the two PPAC's, was used.

Only a tiny fraction, $\sim 10^{-8}$, of the reaction products which passed through the focal plane were from two-body final states, there being a high background of spallation products that reached the detector in a broad momentum band. Therefore, the detection system had to have extremely good particle identification.

Figure 1 shows the A/Q spectrum at $T_p = 186$ MeV. The condition for selecting the correct time-of-flight stop pulse of the cyclotron rf has been applied. The positions of the ^{13}C and ^{13}N ions of the various charge states are indicated. The $^{13}\text{N}^{7+}$ falls on the high side of the

TABLE I. Properties of ^{13}N recoils from the $^{12}\text{C}(p,\pi^0)^{13}\text{N}_{g.s.}$ reaction.

T_p (MeV)	Opening half angle (deg)	T_{recoil} minimum (MeV)	Charge state population (%)			T_{recoil} maximum (MeV)	Charge state population (%)		
			5+	6+	7+		5+	6+	7+
153.5	4.8	10.5	43	43	3	14.8	28	57	11
166.1	7.4	10.4	44	42	3	17.4	21	58	18
186.0	10.0	10.5	43	43	3	21.1	14	56	28
204.0	11.8	10.8	42	44	3	24.6	10	52	37

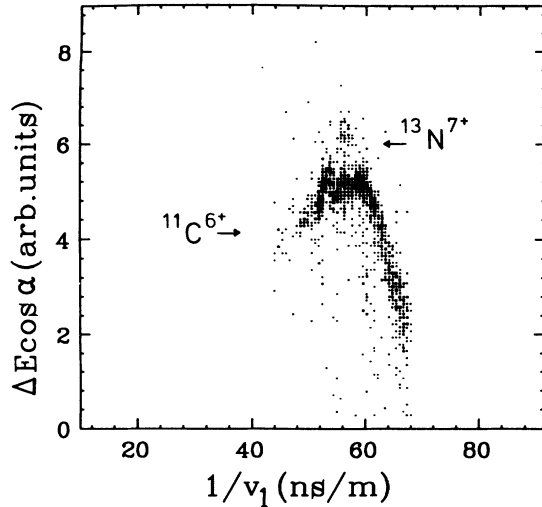


FIG. 2. Two-dimensional histogram of $\Delta E \cos \alpha$ vs $1/v_1$, where ΔE is the energy loss in the proportional counter, α the angle of the ion's velocity vector relative to the focal plane normal, and v_1 the ion's velocity through the QQSP. The cut on the A/Q spectrum accepted ions with $A/Q = 13/7$ and $11/6$. The full and open arrows denote $^{13}\text{N}^{7+}$ and $^{11}\text{C}^{6+}$ ions, respectively.

very much stronger $^{11}\text{C}^{6+}$ peak. In Fig. 2 the angle corrected energy loss in the PC, $\Delta E \cos \alpha$, is plotted against $1/v_1$, for events which fall in a window centered at $A/Q = 13/7$. Most of the events in this window are from $^{11}\text{C}^{6+}$, but the ^{11}C events are distributed over the whole velocity range whereas the ^{13}N events are much more concentrated and are clearly discernible in Fig. 2. The A/Q spectrum of events that fell within a window in the $(\Delta E \cos \alpha, 1/v_1)$ plane where the $^{12}\text{C}(p, \pi^0)^{13}\text{N}$ recoils are expected to lie are shown in Fig. 3. The $11/6$ peak is greatly reduced, and the $13/7$ peak is cleanly separated.

The PC was only useful in identifying ^{13}N from the

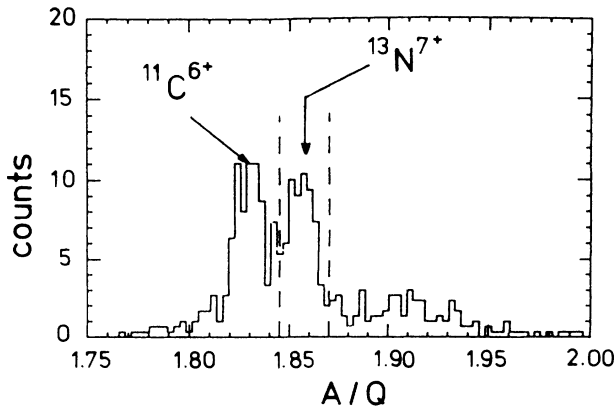


FIG. 3. Spectrum of A/Q near $13/7$. The solid line is the spectrum gated by a window in the $(\Delta E \cos \alpha, 1/v_1)$ plane around the region where the ^{13}N recoils from the $^{12}\text{C}(p, \pi^0)$ reaction are expected.

high momentum branch (π^0 's emitted at backward angles) when α was less than about 46° . At larger angles, the ^{13}N could no longer be separated from carbon because here the nitrogen ions lost so much energy in the foils they were merged into the carbon Bragg curve. For the low momentum branch, some of the ^{13}N recoils did not even reach the PC. However, if the ions reached the second PPAC, their time of flight between the PPAC's and, therefore, their energy after passing through the first set of foils, could be measured. The ^{13}N recoils from reactions in which the pions were emitted at forward angles lost enough energy in the foils that they could be separated by time of flight from ^{13}C ions of the same initial momentum. A scatter plot of events as a function of x vs $1/v_2$, where v_2 is the velocity between the PPAC's, is shown in Fig. 4. It can be seen that the ^{13}C and the ^{13}N are separated. Because the path length through the foils varies considerably with α , and the recoils lost a substantial fraction of their energy in the foils, it was necessary to divide the angular range into six parts in order to affect a clean separation.

Recoil ions from a two-body reaction are located along an elliptically shaped kinematic locus in the (p, θ) plane. The lengths of the axes are determined by the recoils' center-of-mass momentum and, therefore, the size of the ellipse increases with increasing T_p . Ellipses for reactions leading to excited states lie within the ground-state ellipse. The energy loss of the recoils in the target, invariably significant in fixed target experiments, causes a spreading of the ellipses towards lower momenta. The fact that the angle in the nonbend plane was not measured in the present experiment introduced an uncertainty in θ ranging from $\pm 2.9^\circ$ at $\theta = 0^\circ$ to $\pm 0.4^\circ$ at $\theta = 10.6^\circ$.

Figures 5 and 6 show scatter plots α vs x for ^{13}C and

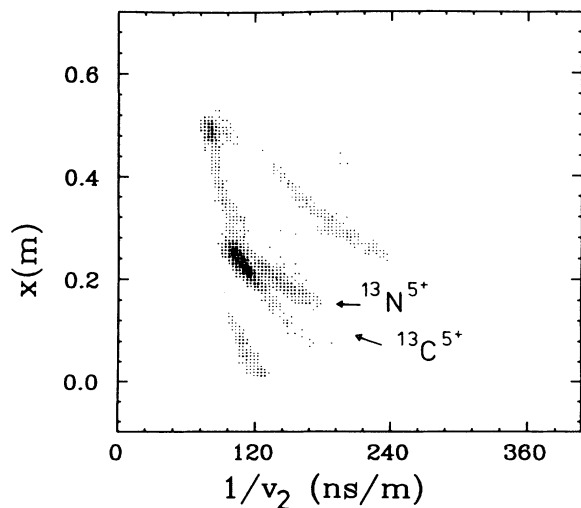


FIG. 4. Two-dimensional histogram of x vs $1/v_2$, where x is the distance along the focal plane (to a good approximation x is proportional to p/Q), and v_2 is the velocity between the two parallel plate avalanche counters. The gate on the A/Q spectrum passed $13/5$ ions, i.e., ^{13}N and ^{13}C in the 5^+ state. These were recoils from the low momentum branch.

^{13}N recoil ions, respectively, at the various T_p . The regions where the (p, π) recoils are expected are indicated. The ^{13}C ground state is not resolved from the three particle stable excited states which are at 3.09, 3.68, and 3.85 MeV; ^{13}N has no bound excited states. The π^0 rest mass is less than that of the π^+ and, therefore, at energies near threshold the $^{12}\text{C}(p, \pi^0)$ ellipse is considerably larger than that for $^{12}\text{C}(p, \pi^+)$. As can be seen in Fig. 6, the $^{12}\text{C}(p, \pi^0)$ reaction is strongly forward peaked in (π^0) angle and at 204 MeV the cross section for producing the higher momenta ^{13}N was so small, ≈ 60 nb/sr (laboratory), that the contributions from the background were significant. Most of the background events were reaction products resulting from the beam halo hitting the vacuum chamber downstream of the target. Also shown in Fig. 6 is the region where events from the high momentum branch of the $^{12}\text{C}(p, \gamma)^{13}\text{N}_{\text{g.s.}}$ reaction would be found. This region does not contain a significant number

of events above background. The recoils corresponding to the forward emitted gamma rays had too short a range to be detected with the present setup.

The differential cross sections, $d\sigma/d\Omega_{\text{c.m.}}$, were obtained from the measured recoil ion angular distribution in the (p, θ) plane. In order to allow for the fact that the angle in the nonbend plane was not measured, an iterative procedure was performed and the true angular distributions $N(\theta)$ extracted from the measured angular distributions using the relationship:

$$N(\theta)d\theta = \kappa(\theta) \sum_{p_{\min}(\theta)}^{p_{\max}(\theta)} n(p_1, \theta)/\epsilon_Q(p), \quad (3)$$

where $\epsilon_Q(p)$ is the probability of recoil with momentum p to be in charge state Q and $\kappa(\theta)$ is the correction needed because only the angle in the bend plane is measured.

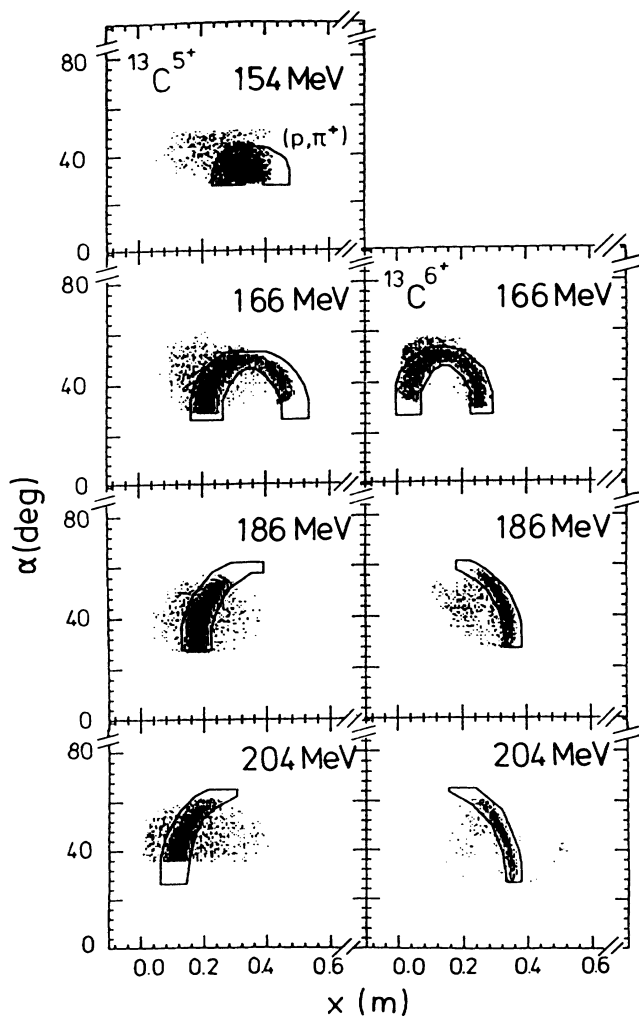


FIG. 5. Two-dimensional histogram in the α vs x plane for ^{13}C ions in the 5^+ state (left-hand side of picture) and the 6^+ state (right-hand side). The solid lines delineate the region where the recoils from the (p, π^+) reaction are expected to fall.

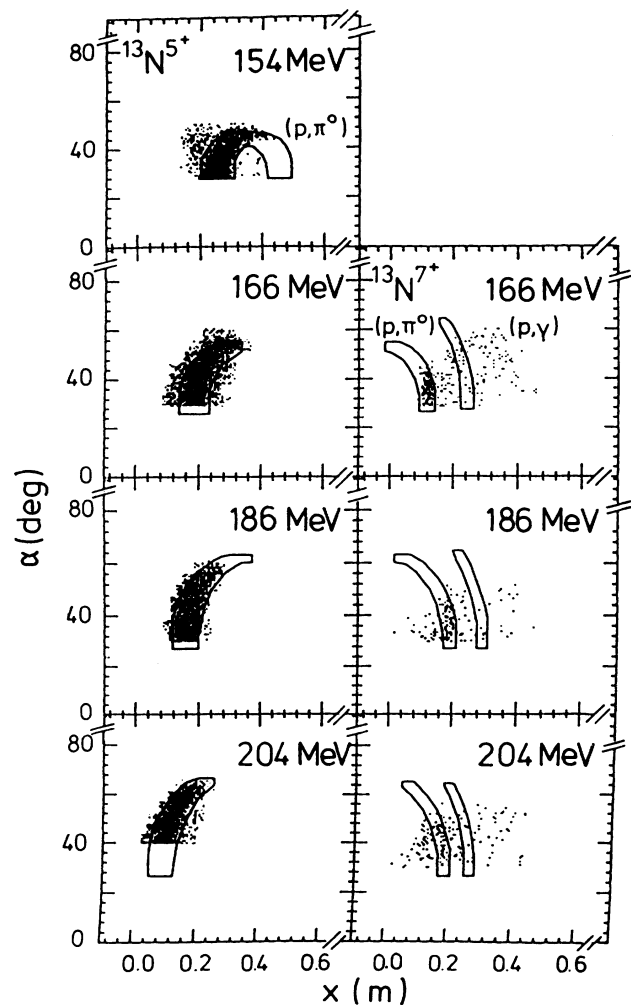


FIG. 6. Two-dimensional histogram in the α - z plane for ^{13}N ions in the 5^+ state (left-hand side of picture) and the 7^+ state (right-hand side). The solid lines delineate the region where the recoils from the (p, π^0) reaction are expected to fall. The position of the high momentum branch of the (p, γ) reaction is also indicated.

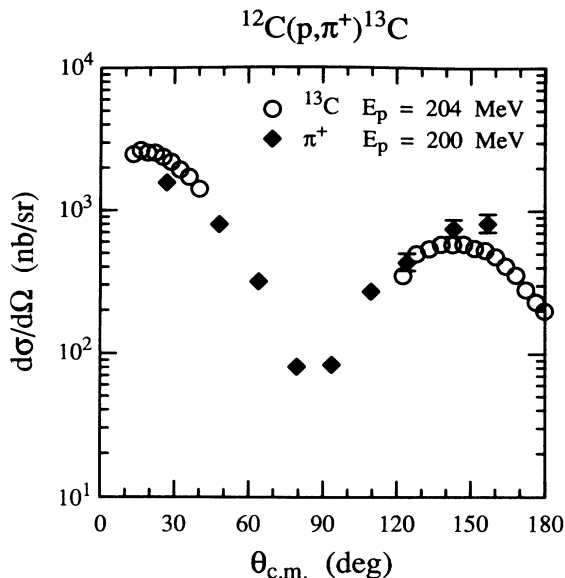


FIG. 7. Differential cross sections for the $^{12}\text{C}(p, \pi^+)^{13}\text{C}$ reaction at 204 MeV (circles) compared with published [8] results at 200 MeV where the π^+ were detected (diamond). Error bars are marked where the statistical error is larger than the symbol size.

The correction $\kappa(\theta)$ depends on the angular distribution and was calculated using the following self-consistent iteration procedure: Starting with $\kappa = 1$, $N(\theta)$ is obtained using Eq. (3). From the angular distribution thus obtained a new n , $n_{\text{sim}}(p, \theta)$, is derived using a Monte Carlo simulation which takes into account the spread in the nonbend plane. From $n_{\text{sim}}(p, \theta)$ and Eq. (3) a new $\kappa(\theta)$ is obtained. The iteration converges within two steps with an accuracy of 1%. The systematic error in $d\sigma/d\Omega$ from uncertainties in ϵ_Q , target thickness, and solid angle is estimated to be about 10%.

As a check, the (p, π^+) cross sections measured here can be compared to those previously reported in experiments where the pion was detected. The energy for which this can be best done is 204 MeV where the present results can be compared to pion data taken [8] at 200 MeV, and the comparison is shown in Fig. 7. The two experiments are in satisfactory agreement at 124° and at 143° . However, at the most forward angle measured in the pion work, 27° , the present work finds a 30% larger cross section while at the most backward (p, π^+) angle, 157° , the present cross section is 40% smaller.

RESULTS

The differential cross sections obtained for the $^{12}\text{C}(p, \pi^0)^{13}\text{N}_{\text{g.s.}}$ reaction are shown in Figs. 8–11. At all bombarding energies ^{13}N ions in the 5^+ charge state were measured for the low momentum branch while at all but the lowest bombarding energy the 7^+ charge state was used for the high momentum branch. At 153.5 MeV it was not possible to separate out the ^{13}N recoils in

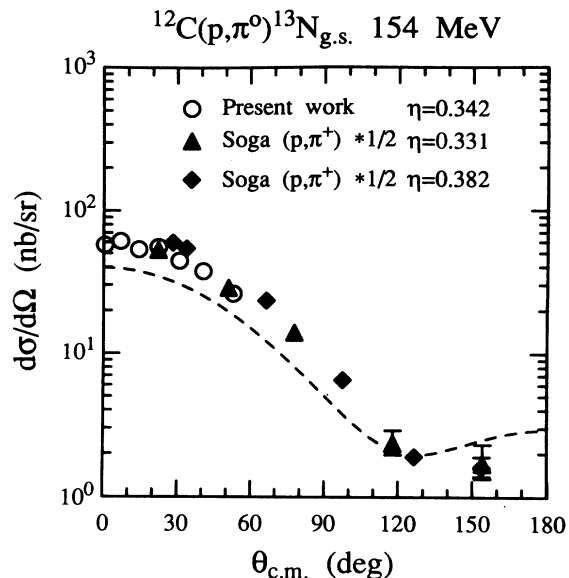


FIG. 8. Differential cross sections for the $^{12}\text{C}(p, \pi^0)^{13}\text{N}$ reaction (circles) at 154 MeV. The solid symbols are the cross sections, divided by 2, for the $^{12}\text{C}(p, \pi^+)^{13}\text{C}_{\text{g.s.}}$ reaction [8,10] at nearby reduced momenta (η). The dashed line is the result of an R matrix calculation using matrix elements given in Ref. [10] from a fit to (p, π^+) data taken at $T_p = 170$ – 190 MeV.

the high momentum branch (where the cross sections are very small). Also shown in Figs. 8–11 are data from the mirror $^{12}\text{C}(p, \pi^+)^{13}\text{C}$ reaction, taken at similar values of reduced momentum in the c.m. system, η , where $\eta = p_\pi/m_\pi c$. The π^+ data have been divided by 2, since isospin invariance requires

$$\frac{d\sigma/d\Omega(p, \pi^+)}{d\sigma/d\Omega(p, \pi^0)} = \frac{(1/2, 1, -1/2, 1 : 1/2, 1/2)^2}{(1/2, 1, 1/2, 0 : 1/2, 1/2)^2} = 2. \quad (4)$$

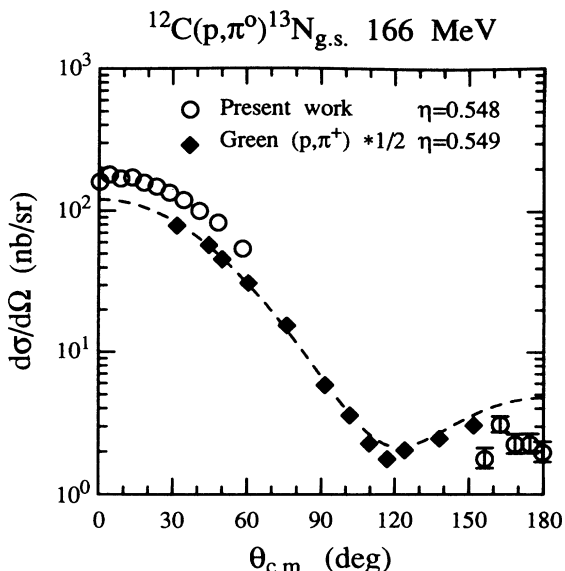


FIG. 9. Same as Fig. 8 at 166 MeV.

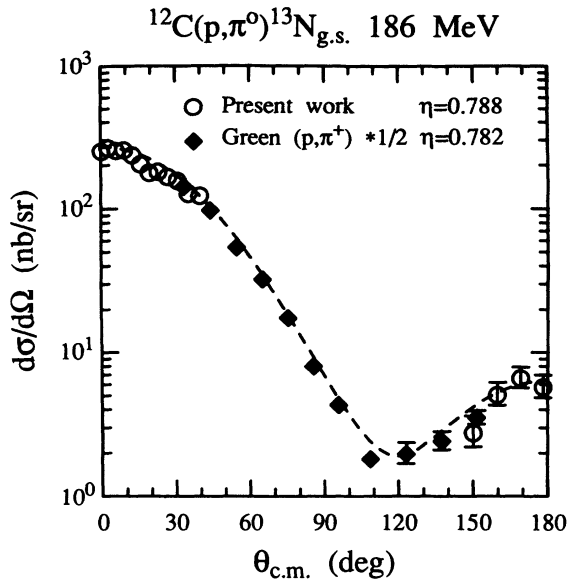


FIG. 10. Same as Fig. 8 at 186 MeV.

The data on the two mirror (p, π) reactions are in very good agreement at 154, 186, and 204 MeV. However, at 166 MeV ($\eta = 0.55$) the (p, π^0) cross sections in the forward direction are about a factor of 1.6 greater than what is expected from the corresponding (p, π^+) values. The angular distributions are sharply peaked forward and, therefore, the total cross sections differ by a similar factor.

Coulomb effects are important near threshold and these were calculated using the R matrix theory of Eisenbud and Wigner [14,15]. For a binary reaction involving states with positive parity and spins 0 and 1/2 in both the entrance and the exit channel, the differential cross

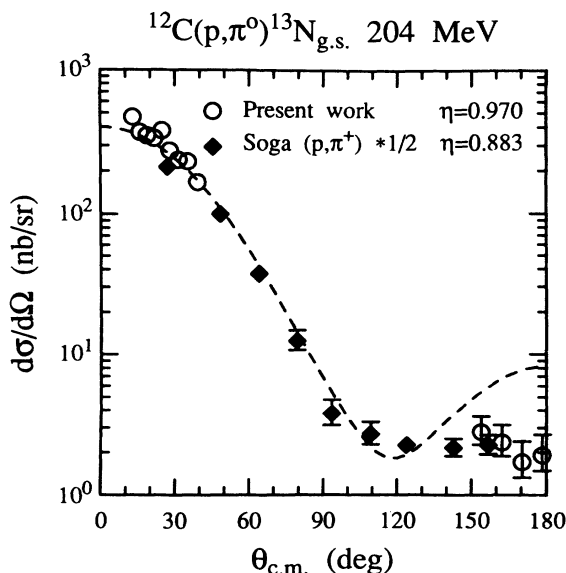


FIG. 11. Same as Fig. 8 at 204 MeV.

section can be written:

$$\frac{d\sigma}{d\Omega} = gg^* + hh^*, \quad (5)$$

where g, g^* and h, h^* are the non-spin-flip and spin-flip scattering amplitudes and their complex conjugates, respectively. The amplitudes g and h can be written as sums of products of scattering matrix elements, T , and Legendre polynomials. Each T matrix element is a product of an energy-independent R matrix element, a phase factor which depends on the charge of the outgoing particle, the Coulomb parameter, λ , and an energy-dependent Coulomb barrier transmission factor. The R matrix elements have been fitted to the π^+ data at 170, 183, and 190 MeV by Green [10]. The T matrix elements for the (p, π^0) reaction have been calculated from these R values after dividing by a factor of 2, according to Eq. (4), and setting $\lambda = 0$. From these T matrix elements $d\sigma/d\Omega$ has been obtained using Eq. (5) and the results are shown as dashed lines in Figs. 8–11.

There are several significant differences between the predicted and measured cross sections. The differential cross sections near 180° decrease by about a factor of 3 between 186 and 204 MeV which, of course, will not be predicted by a calculation using energy-independent matrix elements. It should be noted that this drop is seen in both the (p, π^0) and the (p, π^+) work though, because the recoil experiment measures all the way out to 180° the effect is seen more clearly in the (p, π^0) study. At 166 MeV the (p, π^0) data is poorly fit, as expected because of the anomaly at this energy discussed above. The cross sections for both reactions are underpredicted at 154 MeV.

The total cross sections $\sigma_t (= 4\pi A_0)$ that were obtained from the Legendre polynomial fits are listed in Table II. At $T_p = 153.5, 166.1,$ and 186.0 MeV σ_t for the $^{12}\text{C}(p, \pi^0)^{13}\text{N}_{g.s.}$ reaction can be compared directly with σ_t of the $^{12}\text{C}(p, \pi^+)^{13}\text{C}_{g.s.}$ reaction, because η agrees within 1%. For $\eta = 0.34, 0.55,$ and 0.79 the ratio $\sigma_t(p, \pi^+)/\sigma_t(p, \pi^0)$ is $2.02 \pm 0.14, 3.14 \pm 0.12,$ and 2.12 ± 0.16 , respectively. The total cross section at 166 MeV is therefore 1.57 ± 0.06 larger than predicted by isospin invariance.

In Fig. 12 the values of σ_t for $^{12}\text{C}(p, \pi^0)^{13}\text{N}_{g.s.}$ and $^{12}\text{C}(p, \pi^+)^{13}\text{C}_{g.s.}$ are plotted along with the R matrix calculation results for these two reactions. The (p, π^0) cross sections have been multiplied by 2. A noteworthy feature of the yield curves is that for $\eta < \sim 0.4$ both the

TABLE II. Total cross sections obtained for the $^{12}\text{C}(p, \pi^0)^{13}\text{N}_{g.s.}$ reaction at the various bombarding energies with statistical error. Also shown at each energy is $\eta = p/m_\pi c$, the scaled π^0 momentum in the c.m. system.

T_p (MeV)	η	σ_t (nb)
153.5	0.34	192 ± 8
166.1	0.55	434 ± 12
186.0	0.79	458 ± 22
204.0	0.97	643 ± 31

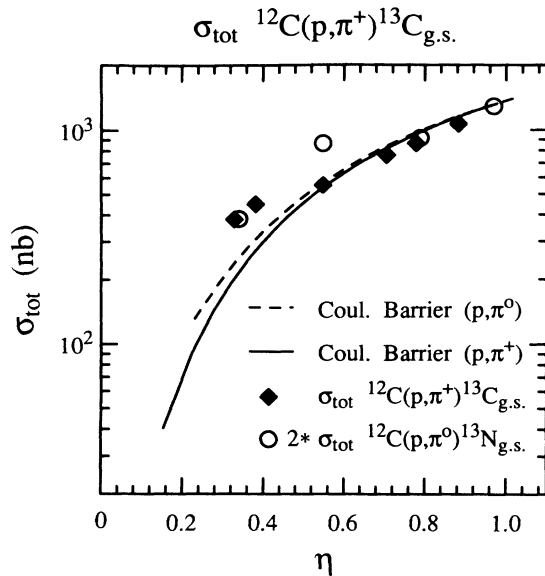


FIG. 12. Total cross sections, as a function of scaled pion momentum, for the $^{12}\text{C}(p, \pi^+)^{13}\text{C}_{g.s.}$ (diamonds) and the $^{12}\text{C}(p, \pi^0)^{13}\text{N}_{g.s.}$ (circles) reactions. The (p, π^0) cross sections have been multiplied by 2. The solid line is the result of a Coulomb barrier calculation, using the matrix elements given in Ref. [10], for the (p, π^+) reaction and the dashed line the result of the same calculation for the (p, π^0) reaction. The statistical errors are smaller than the size of the symbols.

(p, π^0) and (p, π^+) cross sections are substantially greater than the R matrix elements extracted at higher energies would predict. The difference at 154 MeV, shown in Fig. 8, between calculation and experiment is a manifestation of this effect. The reason for the anomalous value of $\sigma(p, \pi^0)/\sigma(p, \pi^+)$ at $\eta = 0.55$ ($T_p = 166$ MeV) is not apparent, and further experiments are needed to confirm this result. Of particular importance would be a determination of the width of any observed structure in this energy region, which is close to the threshold for π^- production.

At 186 and 204 MeV, ^{13}O recoils from the $^{12}\text{C}(p, \pi^-)$ reaction were observed. Only the ground state of ^{13}O is stable against particle emission. Because of the greater energy loss of oxygen ions in the detector foils, only those recoils corresponding to pions emitted in the backward direction were observed. The ^{13}O recoils were best separated at 204 MeV, where the average cross section was found to be 0.68 ± 0.10 nb/sr over the angular range $155^\circ < \theta_{c.m.} < 180^\circ$. No significant variation with angle was observed, within the accuracy of about ± 0.3 nb/sr per 5° interval.

For the $^{12}\text{C}(p, \gamma)^{13}\text{N}$ reaction only recoils accompanying gamma rays emitted in the backward direction would have been observed because the ^{13}N ions from reactions where the gamma rays were emitted forward did not have enough energy to reach the proportional counter. No counts above background were observed in the regions of

the angle-momentum plane where recoils from the radiative capture reaction would be expected. Upper limits of 0.20 nb/sr for gamma rays in the 165° – 180° region could be placed at 166 and 204 MeV; at 186 MeV the upper limit was about 0.5 nb/sr.

There is not much known about radiative capture in this energy region. Measurements of the $^{16}\text{O}(\gamma, p)^{15}\text{N}$ reaction at $T_p = 100$ – 400 MeV have been reported [16] by Leitch *et al.* Taking their results at 135° (their largest angle) and converting to (p, γ) using detailed balance, leads to a cross section for feeding individual states of ≈ 0.1 nb/sr at 200 MeV and ≈ 1 nb/sr at 150 MeV. The most recently published radiative capture calculations are those of McDermott *et al.* [17]. Their code predicts [18] 0.05 nb/sr for the $^{12}\text{C}(p, \gamma)^{13}\text{N}$ cross section in the 160° – 180° region at 200 MeV. The cross section is expected to be much larger in the forward direction and, indeed, the same calculation [18] predicts 20 nb/sr for gamma rays emitted at 0° .

The quality of the present measurements was limited by the relatively large energy loss of the recoil ions in the target. This limitation would not be present in a storage ring, where much thinner targets are used. For this reason, a recoil detection facility is presently being constructed for use on the Cooler Ring at the Indiana University Cyclotron Facility. A second limitation in the present work was caused by the large energy loss of the ions traversing the foils in the detecting system. Much thinner foils, 30–50 $\mu\text{g}/\text{cm}^2$, are now available and will be used in the system that is presently being developed. It should therefore be possible to identify lower-energy recoils, including those accompanying forward emitted gamma rays in the $^{12}\text{C}(p, \gamma)$ reaction.

CONCLUSIONS

Using the recoil detection technique, extensive measurements of a (p, π^0) reaction on a complex nucleus are reported for the first time. In the 150–200 MeV region, the $^{12}\text{C}(p, \pi^0)^{13}\text{N}$ reaction was found to be strongly peaked in the forward (pion) direction with an angular distribution similar to that of the mirror $^{12}\text{C}(p, \pi^+)^{13}\text{C}_{g.s.}$ reaction. At 154, 186, and 204 MeV the ratio of the (p, π^0) to the (p, π^+) cross section is 1:2 as expected from isospin invariance, but at 166 MeV this ratio rises to 1.6:2. The reason for the anomalous behavior at 166 MeV is not known. Both the rapid change in the 180° cross section near 200 MeV and the fact that when the cross sections at higher energies are extrapolated towards threshold in a calculation that includes the effect of the Coulomb barrier the cross sections near $\eta = 0.4$ ($\eta = p_\pi/m_\pi c$) are underpredicted by about a factor of 1.5, suggest an energy dependence of the R matrix elements. At the higher energies, ^{13}O recoils from the $^{12}\text{C}(p, \pi^-)^{13}\text{O}$ reaction were also observed. Upper limits of about 0.2 nb/sr were found for the $^{12}\text{C}(p, \gamma)^{13}\text{N}$ reaction for gamma rays emitted near 180° .

- [1] P. W. F. Alons, R. D. Bent, J. S. Conte, and M. Dillig, Nucl. Phys. **A480**, 413 (1988), and references therein; P. W. F. Alons, R. D. Bent, and M. Dillig, *ibid.* **A493**, 509 (1989); R. D. Bent, P. W. F. Alons, and M. Dillig, *ibid.* **A511**, 541 (1990).
- [2] K. Kume, Nucl. Phys. **A504**, 712 (1989); K. Kume and N. Nose, *ibid.* **A528**, 723 (1991).
- [3] J. J. Domingo, B. W. Allerdycy, C. H. Q. Ingram, S. Rohlin, N. W. Tanner, J. Rohlin, E. M. Rimmer, G. Jones, and J. P. Girardeau-Montaut, Phys. Lett. **32B**, 309 (1970).
- [4] S. Dahlgren, B. Hoistad, and P. Grafstrom, Phys. Lett. **35B**, 219 (1971).
- [5] S. Dahlgren, P. Grafstrom, B. Hoistad, and A. Asberg, Nucl. Phys. **A211**, 243 (1973).
- [6] E. G. Auld, A. Haynes, R. R. Johnson, G. Jones, T. Masterson, E. L. Mathie, D. Ottewell, P. Walden, and B. Tatischeff, Phys. Rev. Lett. **41**, 462 (1978).
- [7] B. Hoistad, P. H. Pile, T. P. Sjoreen, R. D. Bent, M. C. Green, and F. Soga, Phys. Lett. **94B**, 315 (1980).
- [8] F. Soga, P. H. Pile, R. D. Bent, M. C. Green, W. W. Jacobs, T. P. Sjoreen, T. E. Ward, and A. G. Drentje, Phys. Rev. C **24**, 570 (1981).
- [9] G. J. Lolos, E. L. Mathie, P. L. Walden, G. Jones, E. G. Auld, W. R. Falk, and R. B. Taylor, Phys. Rev. C **25**, 1086 (1982).
- [10] M. C. Green, Internal Report No. 83-31, Indiana University, Bloomington, Indiana, 1983 (unpublished).
- [11] W. Schott, W. Wagner, P. Kienle, R. Pollock, R. Bent, M. Fatyga, J. Kehayias, M. Green, and K. Rehm, Phys. Rev. C **34**, 1406 (1986).
- [12] J. Homolka, W. Schott, W. Wagner, W. Wilhelm, R. D. Bent, M. Fatyga, R. E. Pollock, M. Saber, R. E. Segel, and P. Kienle, Phys. Rev. C **38**, 2686 (1988).
- [13] J. Homolka, W. Schott, W. Wagner, W. Wilhelm, R. D. Bent, M. Fatyga, R. E. Pollock, M. Saber, R. E. Segel, P. Kienle, and K. E. Rehm, Nucl. Instrum. Methods **A260**, 418 (1987).
- [14] L. Eisenbud and E. P. Wigner, Phys. Rev. **72**, 29 (1947).
- [15] E. P. Wigner, Phys. Rev. **73**, 1002 (1948).
- [16] M. J. Leitch, J. L. Matthews, W. W. Sapp, C. P. Sargent, S. A. Wood, D. J. S. Findlay, R. O. Owens, and B. L. Roberts, Phys. Rev. C **31**, 1633 (1985).
- [17] J. P. McDermott, E. Rost, J. R. Shepard, and C. Y. Cheung, Phys. Rev. Lett. **61**, 814 (1988).
- [18] J. P. McDermott, private communication.